OncoTargets and Therapy

Dovepress
open access to scientific and medical research

Open Access Full Text Article

ORIGINAL RESEARCH

A Hybrid Glioma Tumor Cell Lysate Immunotherapy Vaccine Demonstrates Good Clinical Efficacy in the Rat Model

This article was published in the following Dove Press journal:
OncoTargets and Therapy

Xin-Long Li[1,2,*]
Shan Zeng[1,2,*]
Hai-Ping He[1,2]
Xu Zeng[1,2]
Li-Lei Peng[1,2]
Li-Gang Chen[1,2]

[1]Department of Neurosurgery, Affiliated Hospital of Southwest Medical University, Luzhou, Sichuan 646000, People's Republic of China; [2]Neurosurgery Clinical Medical Research Center of Sichuan Province, Luzhou, Sichuan 646000, People's Republic of China

*These authors contributed equally to this work

Background: Conventional immunotherapy for glioma is not only expensive but also demonstrates less-than-desired clinical efficacy. In this study, we evaluated the immunotherapeutic efficacy of a tumor cell lysate-based hybrid glioma vaccine developed using a molecular-based approach.

Methods: First, the ability of the autologous (9L-cell lysate) and allogeneic (C6-cell lysate) vaccines against glioma, individually and in combination, to activate Fischer344 rat dendritic cells (DCs) was determined. Next, the activated DCs were co-cultured with T lymphocytes and screened for the optimal DC-to-T-cell ratio. The in vitro efficacy of the DC/T-cell vaccine formulations subjected to different immunogen treatments and co-cultured with glioma cells was evaluated based on glioma cell viability and monocyte chemoattractant protein (MCP)-2 and interferon (IFN)-γ secretion. Subsequently, the efficacy of the 9L + C6 hybrid vaccine was evaluated in 32 glioma rat models, randomly allocated to the following five treatment groups: blank control, tumor, vaccine treatment, thymosin treatment, and vaccine + thymosin treatment (combined treatment). Changes in survival duration, intracranial tumor volume, peripheral blood immune-cell (CD4+ T, CD8+ T, and natural killer [NK] cell) count, and serum cytokine (interleukin [IL]-2, IL-10) levels were assessed in these groups.

Results: The hybrid vaccine demonstrated the highest glioma cell apoptosis and the lowest cell viability and promoted MCP-2 and IFN-γ secretion in vitro. The vaccine treatment and combined treatment groups demonstrated longer survival duration, lower intracranial tumor volume, and higher immune cell glioma tissue infiltration and IL-2 secretion than the untreated tumor group, indicating the vaccine's good in vivo efficacy. Thymosin treatment had minimal effect in enhancing anti-glioma immunity.

Conclusion: We demonstrated the feasibility of combining autologous and allogeneic tumor cell lysates to stimulate specific host cell immune response against glioma cells. The good clinical efficacy of our developed glioma hybrid vaccine in rat models suggests its potential clinical application.

Keywords: tumor cell lysate, vaccine, glioma, molecular simulation, rat, immunotherapy

Correspondence: Li-Gang Chen;
Li-Lei Peng
Department of Neurosurgery, Affiliated Hospital of Southwest Medical University, 25 Taiping Street, Luzhou, Sichuan, People's Republic of China
Email chenligang199066@163.com; lileipeng246@163.com

Introduction

Glioblastoma multiforme (GBM), a highly aggressive glioma subtype, is the most common malignant brain tumor of the central nervous system. The characteristic features of GBM include a high rate of growth, invasiveness, and recurrence.[1] Although the global incidence rate of GBM is relatively low (<10 persons in every 100,000 individuals),[2] the fatality rate within 2 years of diagnosis despite

therapeutic intervention is considerably high. In addition, in 2017, the American Cancer Society reported a dismal 5-year relative survival rate of <10%. Standard therapy for GBM involves surgical resection of the lesion, followed by postoperative chemoradiation. However, this therapy can extend the median survival time by only 8.6 months.[3] Identifying an effective therapeutic approach for GBM is therefore imperative. Importantly, advances in single-cell RNA sequencing technology have enabled the development of a multilayer network biomarker that holds prognostic value in glioma therapy.[4]

In addition to conventional surgery and chemotherapy for gliomas, new advances in immunotherapy have established its potential as a viable alternative. Immunotherapy entails killing of proliferating tumor cells through direct or indirect activation of cytotoxic/lytic T lymphocytes.[5] Foreign antigens, such as tumor cell antigens, are internalized and processed into peptides by the dendritic cells (DCs). These processed peptides are then combined with the major histocompatibility complex (MHC) class-II molecules to form antigen peptide–MHC-II antigen complexes, which are then presented on the surface of DCs. Subsequently, T cells attracted to these complexes engage and participate in the collective immune regulation and immune response process via T-cell receptors (TCRs).[6] DCs have been the focal point of disease vaccine research because of their effective antigen-presenting ability. The heterogenous DCs are categorized on the basis of their functional, morphological, and immunological features [7]. Antigen-presenting DCs bind to the cell surface receptors of both CD4+ and CD8+ T lymphocytes and induce the secretion of cytotoxic/lytic cytokines and chemokines against tumor cells.[7]

The use of tumor-associated antigens, such as peptides, proteins, mRNA, tumor cells, tumor cell lysates, as sources of DC vaccine types is being tested in clinical trials.[8] However, these vaccines have shown reasonable efficacy in promoting immune evasion and tumor progression.[7] Thus, DC vaccines are trending toward application in anticancer combination therapies to improve patient treatment response during early disease stages. For instance, APCEDEN®, an autologous monocyte-derived and tumor lysate-pulsed mature DC-based vaccine with reasonable antitumor efficacy, has been approved for treatment of four cancer types.[7] In addition to the aforementioned conventional types of DC vaccines, other DC-specific immunogenic methods engineered to date include targeted gene editing through CRISPR/Cas9 or RNAi techniques[9] and nanoparticle-based (nanovaccine) strategies, such as the use of the polymer inulin acetate, which is a potent immunogen with minimal undesirable toxicity.[10–12] Furthermore, tumor cell lysate-based nanovaccines have demonstrated effective immunopotentiation of DCs and T cells in melanoma combination immunotherapy.[13]

Conventional immunotherapy, such as CAR-T and PD-1/PD-L1 immunotherapy, and DC vaccines for glioma are not only expensive but also demonstrate less-than-desired clinical efficacy.[14–18] In this study, we focused on improving the conventional tumor cell lysate-based hybrid vaccine to overcome the current problem of poor clinical efficacy. Most published studies have used either autologous or allogeneic antigens, but studies on their combined use are rare. This is a study to use a combination of autologous and allogeneic tumor cell lysates to stimulate specific host cell immune response to target glioma cells. Specifically, we evaluated the formulation of a hybrid glioma vaccine composed of autologous 9L tumor cell lysate and allogeneic C6 tumor cell lysate using a tumor cell lysate-based approach. Autologous tumor cells have cell-surface epitopes nearly similar to those of host tumor cells, whereas allogeneic tumor cells share certain highly conserved epitopes with the host tumor cells.[19] Because of the heterogeneous nature of tumor cells, autologous antigens typically exhibit poor immunogenicity.[19] Allogeneic antigens can elicit a potent cross-immune response to kill tumor cells, causing tumor regression.[19] Therefore, in this study, we included these antigens as adjuvants in the vaccine formulation.

Tumor cell lysate-activated DCs and T lymphocytes were co-cultured to determine the optimal DC-to-T-cell formulation for use as a molecular vaccine against glioma cells cultured in vitro. The cytolytic in vitro efficacy of the three vaccines (autologous, allogeneic, and hybrid) on glioma cells was evaluated. In addition, the in vivo therapeutic effect of the hybrid glioma cell lysate vaccine and the extent of infiltration of peripheral blood immune cells and surrounding tumor immune cells in the 9L/Fischer344 (F344) rat glioma model were assessed. The developed glioma hybrid vaccine demonstrated good clinical efficacy in rat models. Our results provide new insights into glioma clinical therapy.

Materials and Methods

Animal Care and Handling for in vitro DC Primary Cell Culture

Bone marrow-derived DCs were obtained from the femur and tibia of ten 6- to 8-week-old Fischer344 (F344) rats

(Beijing Vital River Laboratory Animal Technology Company, China), each weighing 150–180 g. The rats were bred in the experimental animal facility in the Clinical Research Center, Southwest Medical University, China. For in vitro experiments, the rats were killed by cervical dislocation. The bone marrow cavity was then washed with phosphate-buffered saline (PBS), centrifuged, and resuspended to obtain the DC suspension. Next, a lymphocyte-separation medium was added to the DC suspension and centrifuged to enable aspiration of the middle bone marrow stromal cell layer (white membrane layer). The aspirate was then cultured under sterile conditions in a DC-cell RPMI-1640 growth medium supplemented with 16% v/v fetal bovine serum (FBS), 25 ng/mL GM-CSF, 25 ng/mL interleukin (IL)-4, and 100 U/mL penicillin + 100 U/mL streptomycin at 37ºC in a 5% CO_2 humidified incubator. Cell growth was monitored every day until the last day of the experiment. All experimental procedures were approved by the Institutional Animal Care and Use Ethics Committee at the Southwest Medical University, China, and were conducted in accordance with the Laboratory Animal Guidelines for Ethical Review of Animal Welfare.

Flow Cytometric Detection of Cell Marker Expression on Isolated DCs

To prepare the in vitro molecular dynamics-based glioma vaccine, we first tested five immunogens—PBS, 9L rat glioma cell lysate (Shanghai EK-Bioscience, China), C6 rat glioma cell lysate (Cyagen Biosciences, China), 9L + C6 rat glioma cell lysate (mixed cell lysate), and lipopolysaccharide (LPS; Sigma, USA)—for their ability to activate F344 rat bone marrow-derived DCs. Each of the immunogen was incubated in vitro with primary F344 DCs for 72 h at 37°C in a 5% CO_2 humidified incubator. Suspensions of 70%–80% confluent glioma cell lysates were co-cultured with primary DCs. These cultured DCs, before and after the respective treatments, were isolated by centrifugation and resuspended to obtain single-cell suspensions (50 µL; about 1×10^6 cells) for flow cytometric analyses (BD FACSuite™ software, BD Biosciences, USA). Subsequently, the single-cell suspensions were incubated with CD80, CD86, OX62, OX6, CD11c, and MHC-II antibodies (eBioscience, USA) for 30 min at 25°C in the dark before submitting to flow cytometry (BD Biosciences, USA).

Detection of T-Lymphocyte Proliferation in Rat Spleen

The F344 rats were killed, and their spleens were removed under sterile conditions. After grinding the spleen with the plunger of a 5-mL syringe, the isolated T lymphocytes were added to 2 mL of lymphocyte separation solution before submitting to centrifugation at 2000 rpm for 20 min at room temperature. The lymphocyte layer (white membrane in the middle of the tube) was aspirated, washed thoroughly, and cultured at 37°C in a 5% CO_2 humidified incubator. To detect cell proliferation, the T-cell suspension was incubated with an equal volume of carboxyfluorescein succinimidyl ester (CFSE) working solution at 37°C for 10 min. The reaction was terminated by adding 40% cold fetal calf serum and incubating it for 10 min. The T-cell suspensions, thus obtained, were washed twice before resuspending in a complete culture medium. Next, the T-cell suspensions were co-cultured with activated DCs at the DC-to-T-cell target ratios of 0:1, 1:5, 1:10, 1:20, 1:40, and 1:80 for 3 days before submitting to flow cytometry. The T-cell proliferation index was then calculated using the FlowJo™ flow cytometry software (BD Biosciences, USA).

Detection of Glioma-Cell Apoptosis

The best DC-to-T-cell target ratio was selected for co-culture with glioma cells at glioma-to-DC/T-cell target ratios of 10:1, 20:1, and 50:1. Glioma cells in the logarithmic growth phase were seeded onto a 96-well plate at 1×10^4 cells/well. After adherence of the seeded glioma cells, the DC/T-cell mixed suspensions at the best DC-to-T-cell target ratio were added to obtain glioma-to-DC/T-cell target ratios of 10:1, 20:1, and 50:1. The five immunogens—PBS (equal volume added to the cells in a well), 9L cell lysate, C6 cell lysate, 9L + C6 mixed cell lysate, and LPS (1 µg)—were then added to each well containing glioma, dendritic, and T cells and incubated for 72 h. The cell lysates (1×10^6 cells) of each group were added to 150 µL of sterile distilled water and centrifuged at 10,000 rpm for 10 min.[20] Annexin V-FITC binding solution (190 µL; BD Biosciences, USA) was added to gently resuspend the cells (5×10^4 to 1×10^5), followed by addition of 5 µL of Annexin V-FITC, which was gently mixed with the cells before incubation at room temperature for 10 min in the dark. Next, propidium iodide staining solution (10 µL; Sigma, USA) was gently mixed with the cell suspension and incubated in an ice bath in the

dark. The resultant suspension was immediately submitted to flow cytometry. The Annexin V-FITC-stained cells appeared green and the propidium iodide-stained cells appeared red. The apoptotic rate of the five treatment groups was calculated using the FACSuite™ flow cytometry software (BD Biosciences, USA). The best glioma cell-to-DC/T-cell target ratio was finally selected to assess the in vitro efficacy of the DC-based vaccine.

Glioma Cell Viability Assay

Glioma cell viability was assessed to determine the in vitro efficacy of the DC-based vaccine. The CCK-8 kit (Sigma, USA) was used to examine the viability of glioma cells in the five treatment groups of DC-activated T cells co-cultured with glioma cells. For this assay, 9L or C6 cells (1×10^4 cells/well) in the logarithmic phase were seeded onto 96-well plates at the respective target ratios of 10:1, 20:1, and 50:1. Co-cultures of DCs and T cells in the tested DC-to-T-cell target ratios in each well were incubated with the CCK-8 (10 μL) solution for 1–4 h. Next, the absorbance (Å) at 450 nm, which indirectly reflects the number of live cells, was measured using a microplate reader. The cell viability was calculated using the following formula:

Cell viability (%) = [A (experimental group) − A (blank group)]/[A (control group) − A (blank group)] × 100%.

ELISA-Based Detection of T-Lymphocyte Chemokine and Cytokine Secretion

Chemokine (monocyte chemoattractant protein [MCP]-2) and cytokine (interferon [IFN]-γ) secretion from T cells for the five treatment groups of DC-activated T cells co-cultured with glioma cells was also assessed as part of the evaluation of the in vitro efficacy of the DC-based vaccine. Lymphocyte chemokine and cytokine secretion in the supernatant was detected after 7 days of co-culture by using the ELISA kit (MCP-2: Beijing Ruike Biotechnology Co. Ltd., China; IFN-γ: MultiSciences [Lianke] Biotech Co. Ltd., China), according to the manufacturers' instructions. The absorbance at 450 nm was measured using a microplate reader.

Animal Grouping for in vivo Experiments

Forty 6- to 8-week-old F344 rats (Beijing Vital River Laboratory Animal Technology Company, China), each weighing 160–180 g, were randomly allocated to five groups (n = 8 per group): saline was microinjected to the brain to establish the animal model for the blank control group, whereas glioma tumor cells were injected into the brain via the same method for the remaining four groups to establish the tumor models (tumor-negative control group; 9L + C6 [9L + C6 mixed cell lysates vaccine] treatment group; thymosin treatment group; and 9L + C6 + thymosin treatment group). Following the establishment of rat glioma models, the blank control and the tumor groups were each treated with 10 μL of normal saline; the 9L + C6 and the 9L + C6 + thymosin treatment groups were each subcutaneously injected with the molecular dynamics-based glioma vaccine on postoperative day 1; and the thymosin and 9L + C6 + thymosin treatment groups were each treated with 0.8 mg/kg thymosin via subcutaneous injection on postoperative day 1, followed by the injection every 3 days.[21] All experimental procedures and studies were approved and performed according to the Institutional Animal Care and Use Committee at the Southwest Medical University, China.

Preparation of Glioma-Cell Suspension for Transplantation into Rat Models

C6 and 9L glioma cells cultured in a complete glioma medium at 80% confluency were harvested to prepare respective single-cell suspensions (1×10^6/10 μL concentration). Trypan blue staining was performed to assess cell viability (target > 90%) of the single-cell suspension, which was temporarily stored at 4°C if not used immediately. 9L and C6 cells, each at a concentration of 3×10^5 cells, were mixed with 100 μL of PBS to prepare 9L and C6 glioma cell suspensions, respectively. Subsequently, the cell suspensions were transplanted into rats to establish glioma.

Establishment and Treatment of 9L/F344 Rat Glioma Models

Each F344 rat was anesthetized with sodium pentobarbital and fixed on an operating table of a stereotactic instrument. After trimming the animal's head hair and disinfecting it, the skin along the midline of the scalp was incised to expose the anterior condyle. A 1-mm-diameter hole was drilled in the bone 0.5 mm before the anterior condyle and 3 mm to the right of the sagittal suture. Care was taken not to damage the dura while drilling. The uniformly mixed glioma cell suspension (10 μL) was delivered into the hole via microinjection within 15 min. The microinjection needle was inserted 6 mm vertically through the hole in the

bone and was slowly pulled out of the hole 10 min after the completion of the injection. Antibiotics were sprayed at the surgical site and the incision was sutured. One day after successfully establishing the tumor-bearing 9L/F344 rat glioma model, the 40 rats in the five treatment groups were administered the aforementioned treatments.

Blood Collection for the Measurement of Blood Cell Count and Cytokine Level

Blood was collected from the tail vein of each rat 1 day before treatment and at 30 days after treatment to analyze blood cell (CD4+ T, CD8+ T, natural killer [NK]) count and cytokine (IL-2 and IL-10) level in sera using flow cytometry and ELISA, respectively. The tails were cleaned and sterilized with alcohol before collecting 70 μL of whole blood. The anticoagulant EDTA was immediately added to the whole blood collected. T-cell (CD3, CD4, CD8) and NK-cell (CD161) antibodies (BD Biosciences, USA) and absolute counting microspheres (BD Biosciences, USA) were incubated for 15 min in the dark before incubation with 50 μL of blood cell lysate and for another 15 min in the dark. The mixture was centrifuged at 1000 rpm for 5 min before submitting to flow cytometry. The remaining whole blood was left at room temperature for 30 min before centrifuging at 1000 *g* for 15 min. The supernatant (200 μL) was then frozen and stored at −20°C. IL-2 and IL-10 concentrations in sera (supernatant samples) were measured using the ELISA kit (Abcam, UK), according to the manufacturer's instructions.

Magnetic Resonance Imaging Examination of Tumor Volume and Survival Status of Rat Models

Magnetic resonance imaging (MRI) examination was performed at 5, 20, 30, and 40 days after surgery to observe the changes in the intracranial tumor volume. First, the rats were injected with pentobarbital. Next, 0.5 mL of glucosamine was injected into the rat's tail vein for contrast-enhanced MRI scans (Philips Achieva 3.0T MRI, Philips Healthcare, Best, The Netherlands). One rat from each treatment group was killed before treatment and after treatment (20 and 30 days after surgery) via excessive pentobarbital injection. The change in glioma intracranial tumor volume was calculated using the Cavalieri formula.[22] Only objective, not subjective, differences in tumor volume were considered for the calculation. The changes in survival duration of rats in each treatment group were observed everyday up to 40 days or till death, whichever was earlier.

Immunohistochemistry

One rat from each treatment group was killed before treatment and after treatment (20 and 30 days after surgery) via excessive pentobarbital injection. After tissue sectioning, the abundance of CD4+ T, CD8+ T, and NK cells around the tumor site was examined by immunohistochemistry. The fixed tissue was dehydrated and embedded before sectioning. The dewaxed sections were placed in a dyeing tank containing 3% methanol and hydrogen peroxide at room temperature for 10 min. The sections were then washed three times with PBS for 5 min each before immersing in 0.01 M citrate buffer solution (pH 6.0). Next, the sections were heated in a microwave oven until boiling and then cooled for 5 min before repeating the process another time. The sections were then washed with PBS two times, each for 5 min, before incubating with goat serum blocking solution at room temperature for 20 min. Subsequently, the sections were incubated with primary antibodies at 4°C overnight, followed by incubation with biotinylated secondary antibodies at 37°C for 30 min. After washing the sections with PBS three times, the 3,3′-diaminobenzidine (DAB) staining reagent (concentrated DAB kit, K135925C, Beijing Zhongshan Jinqiao Biological Co., Ltd., China) was added and the color development was monitored using a light microscope. Excess DAB stain was removed by washing the sections with distilled water (usually after 2 min of staining), followed by the application of hematoxylin as a counterstain. The stained sections were dehydrated, mounted, and sealed with a neutral gum. The sections were first observed at 100× magnification to select the fields of view using an optical microscope (BA200 digital trinocular micro-camera system, McAudi Industrial Group Co., Ltd., China). Images from three fields of view at 400× magnification were then collected. The optical density (integrated optical density [IOD]) and area of all the collected images were measured using the Image-Pro Plus 6.0 image analysis system (Media Cybernetics, Inc., USA), and the average optical density (mean density [MD]) of each image was calculated. The average optical density of each sample was obtained using the average optical density of three images. The average was analyzed by single factor analysis of variance (one-way ANOVA) using the SPSS21 software (SPSS Inc, Chicago, IL, USA) and data are expressed as mean ± standard deviation (SD).

Statistical Analysis

Data from three independent experiments (n = 3) were analyzed using SPSS v21.0 (SPSS Inc, Chicago, IL, USA) and are expressed as mean ± SD. A comparison among different groups was performed using multivariate one-way ANOVA analyses. Values of $p < 0.05$ were considered statistically significant.

Results

Activation of DCs by Glioma-Cell Lysate

To determine the immunogenic effect of DCs on glioma cell lysate, we examined the changes in expression levels of the DC cell-surface markers CD80, CD86, OX62, OX6, CDIIC, and MHC-II. Individual glioma cell lysates, C6 and 9L, and C6 + 9L were tested. The PBS- and LPS-treatment groups were used as experimental controls. Significantly higher expression levels were noted for most of the cell surface markers, except for CD86, after DC treatment (Figure 1). Importantly for most markers, the LPS-treated group (positive control) demonstrated the most significant increase and the PBS-treated group (baseline control) demonstrated the least significant increase in cell-surface markers compared with the other four groups. Moreover, the 9L + C6 group demonstrated a more significant increase than the individual lysates C6 and 9L groups. The results indicate that all treatment methods tested could successfully promote DC maturation and antigen-presentation ability. In addition, the glioma cell lysates, both individual and combined, were able to successfully activate DCs.

Induction of T-Cell Proliferation by DC-to-T Cells at 1:20 Ratio

After successfully confirming DC activation by all the three glioma cell lysates (autologous, allogeneic, and hybrid), we investigated the in vitro co-culture DC-to-T-cell ratio for establishing the vaccine formulation. The six DC/T-cell co-culture groups (0:1, 1:5, 1:10, 1:20, 1:40, and 1:80) stimulated with the glioma cell lysate immunogen were submitted to flow cytometry to assess T-cell proliferation. Different T-cell proliferation capabilities were noted for different groups tested (Figure 2). The

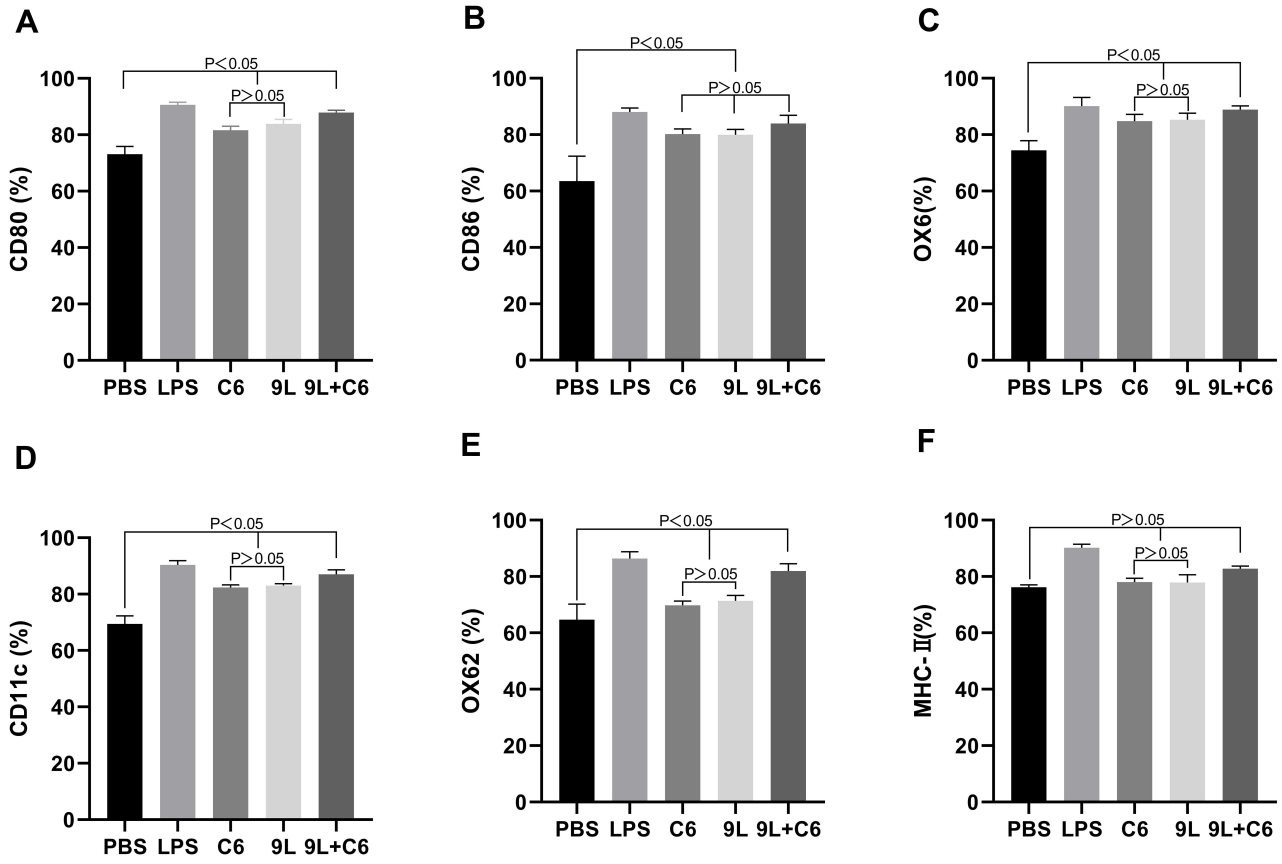

Figure 1 Histograms showing the percentage change in DC cell surface markers (**A**) CD80, (**B**) CD86, (**C**) OX6, (**D**) CD11c, (**E**) OX62, and (**F**) MHC-II. Data are presented as mean ± standard deviation (SD) of three independent experiments (n = 3). One-way ANOVA statistical test was performed for comparisons among groups.

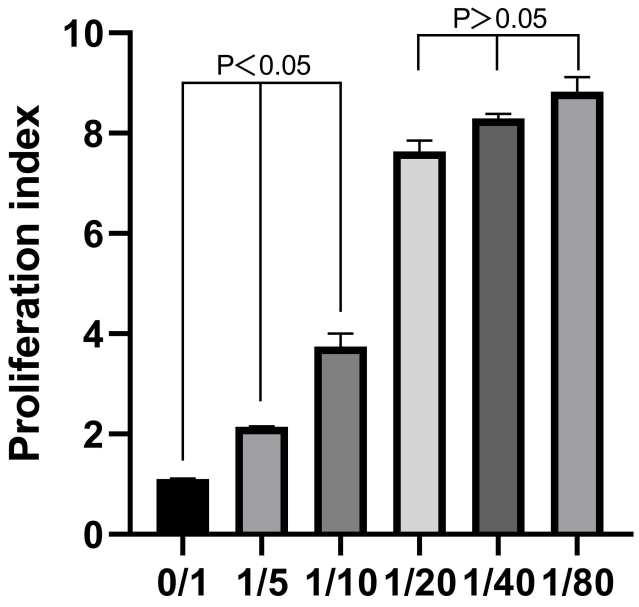

Figure 2 T-cell proliferation index of the six different DC-to-T-cell ratios derived from flow cytometric cell sorting and detection. Data are presented as mean ± standard deviation (SD) of three independent experiments (n = 3). One-way ANOVA statistical test was performed for comparisons among groups.

T-cell proliferation index for the 0:1, 1:5, 1:10 groups was statistically significant ($p < 0.05$), whereas that for the 1:20, 1:40, and 1:80 groups were not significant. We used the DC-to-T-cell ratio of 1:20 for all subsequent experiments because this group demonstrated optimal values to induce sufficient T-cell proliferation.

Induction of Glioma-Cell Apoptosis by a Tumor Cell Lysate-Based 9L + C6 Hybrid Vaccine

The efficacy of the tumor cell lysate-based vaccines was examined by their effect on glioma cell apoptosis. We analyzed three glioma-to-vaccine ratios (10:1, 20:1, and 50:1) for the five treatment groups. At the 10:1 effect target ratio on the apoptotic rate, no significant difference was noted between the 9L lysate and PBS groups ($p > 0.05$); significantly higher rate ($p < 0.05$) was noted in the C6 lysate and mixed (9L + C6) lysate groups than in the PBS group; and no significant difference was noted between the C6 lysate and mixed lysate groups ($p > 0.05$) (Figure 3A). At both 20:1 and 50:1 target ratios, all the three experimental groups (9L, C6, and 9L + C6 treatment groups) demonstrated a higher apoptotic rate than the PBS group (Figure 3B–C; $p < 0.05$). For the mixed cell lysate group, the apoptotic rate increased with an increase in the target ratio ($p < 0.05$). The group also demonstrated a significantly higher apoptotic rate than the 9L- and C6-treatment groups (Figure 3D; $p < 0.05$).

Reduction of Glioma Cell Proliferation by a Tumor Cell Lysate-Based 9L + C6 Hybrid Vaccine

Subsequently, we assessed the efficacy of the tumor cell lysate-based DC vaccines on glioma cell viability at the same three target ratios, 10:1, 20:1, and 50:1, for the five treatment groups. The three experimental treatment groups (9L, C6, and 9L + C6 cell lysate groups) demonstrated a statistically significant decrease in glioma cell viability compared with the PBS group at all three target ratios tested (Figure 4A–C; $p < 0.05$). The mixed cell lysate group demonstrated the least glioma cell viability ($p < 0.05$), which decreased with the increase in the target ratio (Figure 4D; $p < 0.05$).

Induction of T-Lymphocyte Chemokine and Cytokine Secretion by a Tumor Cell Lysate-Based 9L + C6 Hybrid Vaccine

The T-lymphocyte chemokine (MCP-2) and cytokine (IFN-γ) secretion were also evaluated to assess the efficacy of the tumor cell lysate-based vaccine. The 9L group demonstrated no significant difference in MCP-2 and IFN-γ secretion from the PBS group at all three target ratios (Figure 5A–C and 6A-C; $p > 0.05$), whereas the C6 and 9L + C6 groups demonstrated significantly higher MCP-2 and IFN-γ secretion than the PBS group at all three target ratios (Figure 5A–C and 6A-C; $p < 0.05$). Increased MCP-2 and IFN-γ secretion with an increase in the target ratio was noted in the 9L + C6 group (Figures 5D and 6D; $p < 0.05$), indicating that using the mixed glioma lysate as a vaccine immunogen can induce T-cell chemokine and cytokine secretion.

Longer Survival Duration of Tumor-Bearing Rats Treated with the Tumor Cell Lysate-Based Hybrid Vaccine

First, the in vitro efficacy of the tumor cell lysate-based hybrid vaccine (9L + C6 cell lysates as an immunogen) on apoptosis and viability of glioma cells, as well as induction of T-cell chemokine and cytokine secretion, was examined. Then, the in vivo efficacy of the vaccine was investigated on tumor-bearing rat models. The survival of tumor-bearing rats in the four treatment groups (tumor group, 9L + C6

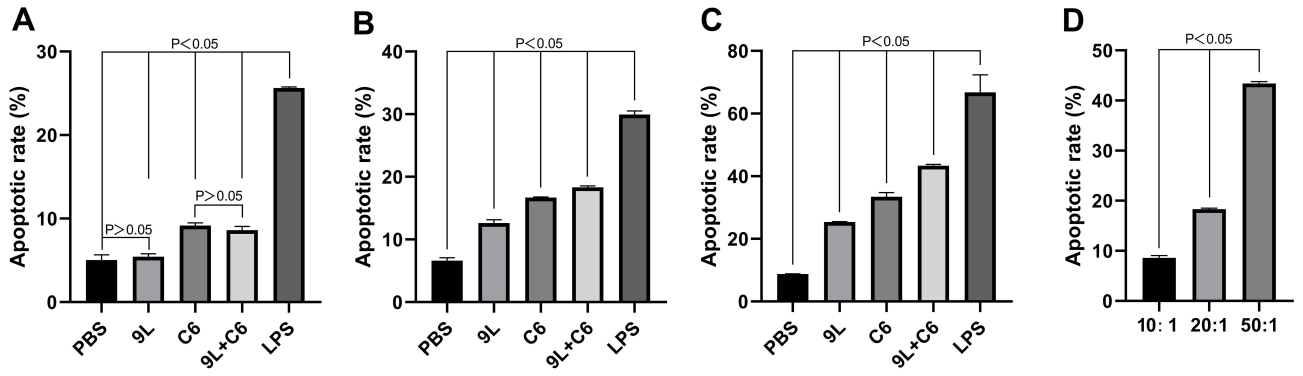

Figure 3 The apoptotic rate (%) of glioma cells at (**A**) 10:1, (**B**) 20:1, and (**C**) 50:1 glioma-to-vaccine ratios for the five DC activation treatment groups and at (**D**) the three target ratios for the 9L + C6 mixed cell lysate group. Data are presented as mean ± standard deviation (SD) of three independent experiments (n = 3). One-way ANOVA statistical test was performed for comparisons among groups.

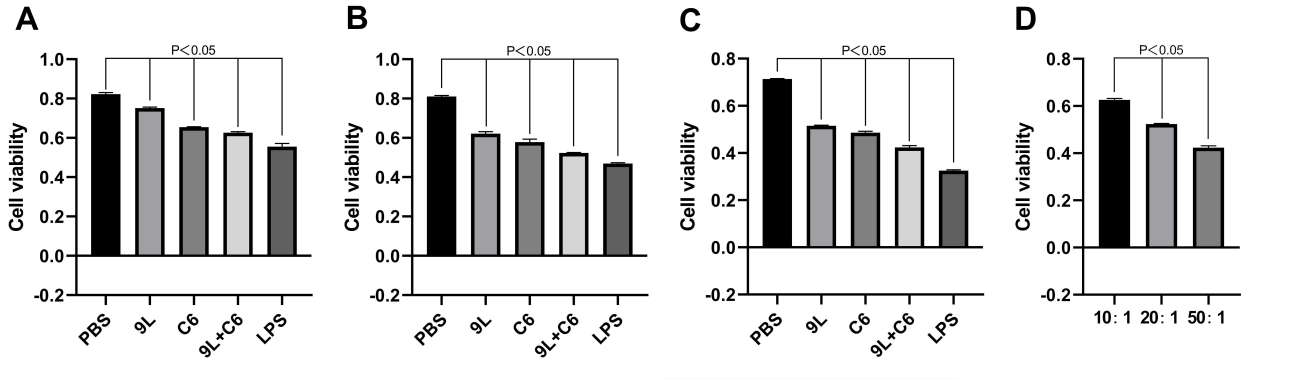

Figure 4 Cell viability of glioma cells at (**A**) 10:1, (**B**) 20:1, and (**C**) 50:1 target ratios for the five dendritic cell (DC) activation treatment groups, and at (**D**) different target ratios for the 9L + C6 treatment group. Data are presented as mean ± standard deviation (SD) of three independent experiments (n = 3). One-way ANOVA statistical test was performed for comparisons among groups.

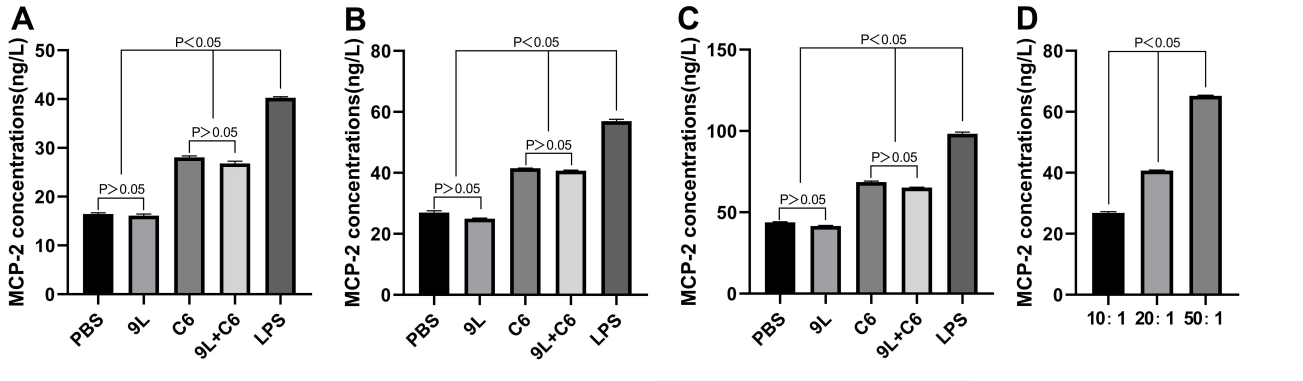

Figure 5 Monocyte chemotactic protein-2 (MCP-2) concentrations at (**A**) 10:1, (**B**) 20:1, and (**C**) 50:1 target ratios for the five DC activation treatment groups, and at (**D**) different target ratios for the 9L + C6 treatment group. Data are presented as mean ± standard deviation (SD) of three independent experiments (n = 3). One-way ANOVA statistical test was performed for comparisons among groups.

treatment group, thymosin-treatment group, and 9L + C6 + thymosin treatment group) over a 60-day period was studied. Both the 9L + C6 and 9L + C6 + thymosin treatment groups demonstrated significantly longer survival duration than the tumor and thymosin-treatment groups (Figure 7; $p < 0.05$). No statistically significant difference in the survival duration was found between the tumor and thymosin-treatment groups (Figure 7; $p > 0.05$).

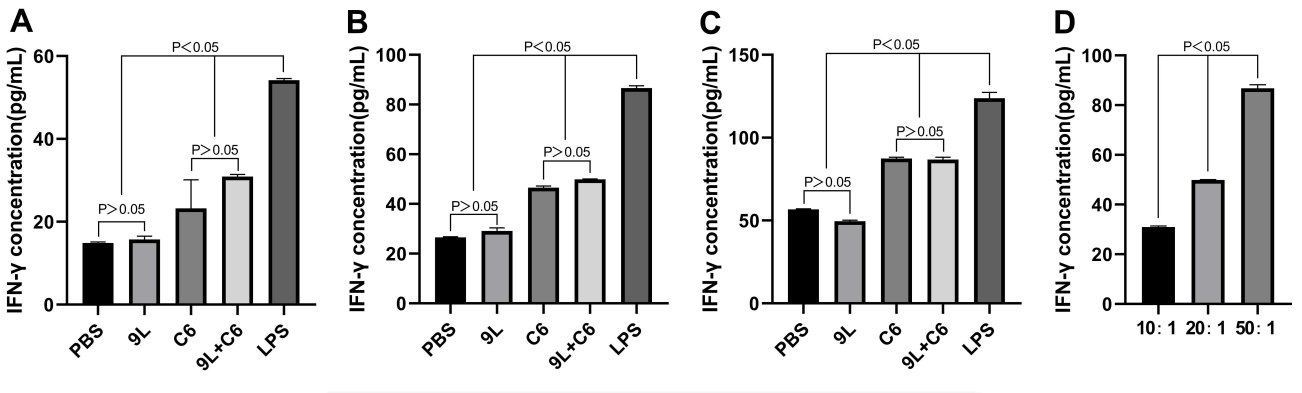

Figure 6 Interferon-gamma (IFN-γ) concentrations at (**A**) 10:1, (**B**) 20:1, and (**C**) 50:1 target ratios for the five dendritic cell (DC) activation treatment groups, and at (**D**) different target ratios for the 9L + C6 treatment group. Data are presented as mean ± standard deviation (SD) of three independent experiments (n = 3). One-way ANOVA statistical test was performed for comparisons among groups.

Reduction of Intracranial Tumor Volume in Tumor-Bearing Rats Treated with a Tumor Cell Lysate-Based Hybrid Vaccine

We also assessed the change in the intracranial tumor volume over a 40-day period in tumor-bearing rats of the four treatment groups through enhanced MRI. All rats initially demonstrated enhanced mass shadows on the right caudate nucleus on day 5, indicating the successful establishment of the tumor. The intracranial tumor volume in the tumor group gradually increased until the rats died (Figure 8A). As the rats in the tumor group did not survive up to day 40, the images for days 5, 10, 20, and 30 are presented. Similarly, the tumor volume in the thymosin-treatment group gradually increased until the rats died (Figure 8C). In contrast, a gradual decrease in tumor volume was noted in the 9L + C6 and 9L + C6 + thymosin treatment groups from days 20 to 40 (Figure 8B and 8D).

Hybrid Vaccine Treatment-Induced Increase of Peripheral Blood CD4+ T- and NK-Cell Count

We investigated the changes in peripheral blood CD4+ T, CD8+ T, and NK cell count in the five treatment groups. The tumor group demonstrated a statistically significant decrease in CD4+ and CD8+ T cells ($p < 0.05$), whereas the NK cell count was higher than that in the blank control group (Figure 8). Higher CD4+ T and NK cells were observed in the 9L + C6 and the 9L + C6 + thymosin treatment groups (Figure 9A; $p < 0.05$), whereas no significant difference was observed in the CD8+ T-cell count compared to the blank control group. No significant difference in $CD8^+$ T-cell count was observed in the 9L + C6, thymosin, and 9L + C6 + thymosin treatment groups compared with the blank control group (Figure 9B). Both the 9L + C6 and 9L + C6 + thymosin treatment groups demonstrated higher CD4+ T- and NK-cell count than the blank control group (Figure 9A and C).

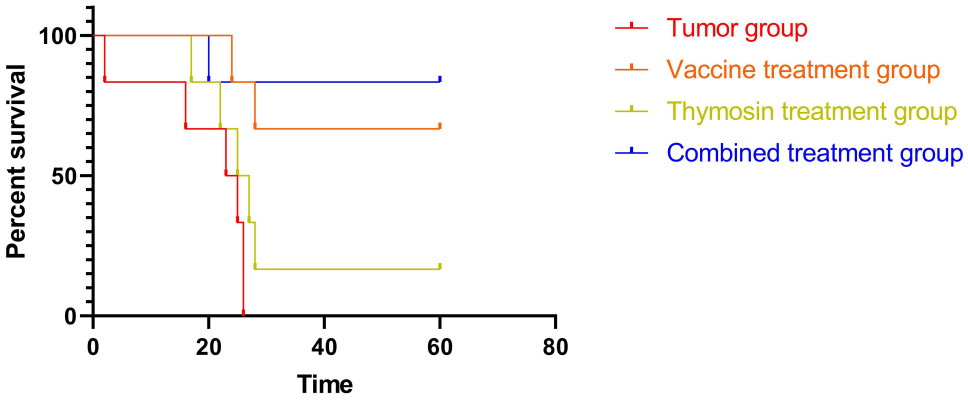

Figure 7 Survival curves of glioma rat models for the four treatment groups (tumor, 9L + C6, thymosin, and 9L + C6 + thymosin groups) over a period of 60 days. Data are presented as mean ± standard deviation (SD) of three independent experiments (n = 3). One-way ANOVA statistical test was performed for comparisons among groups.

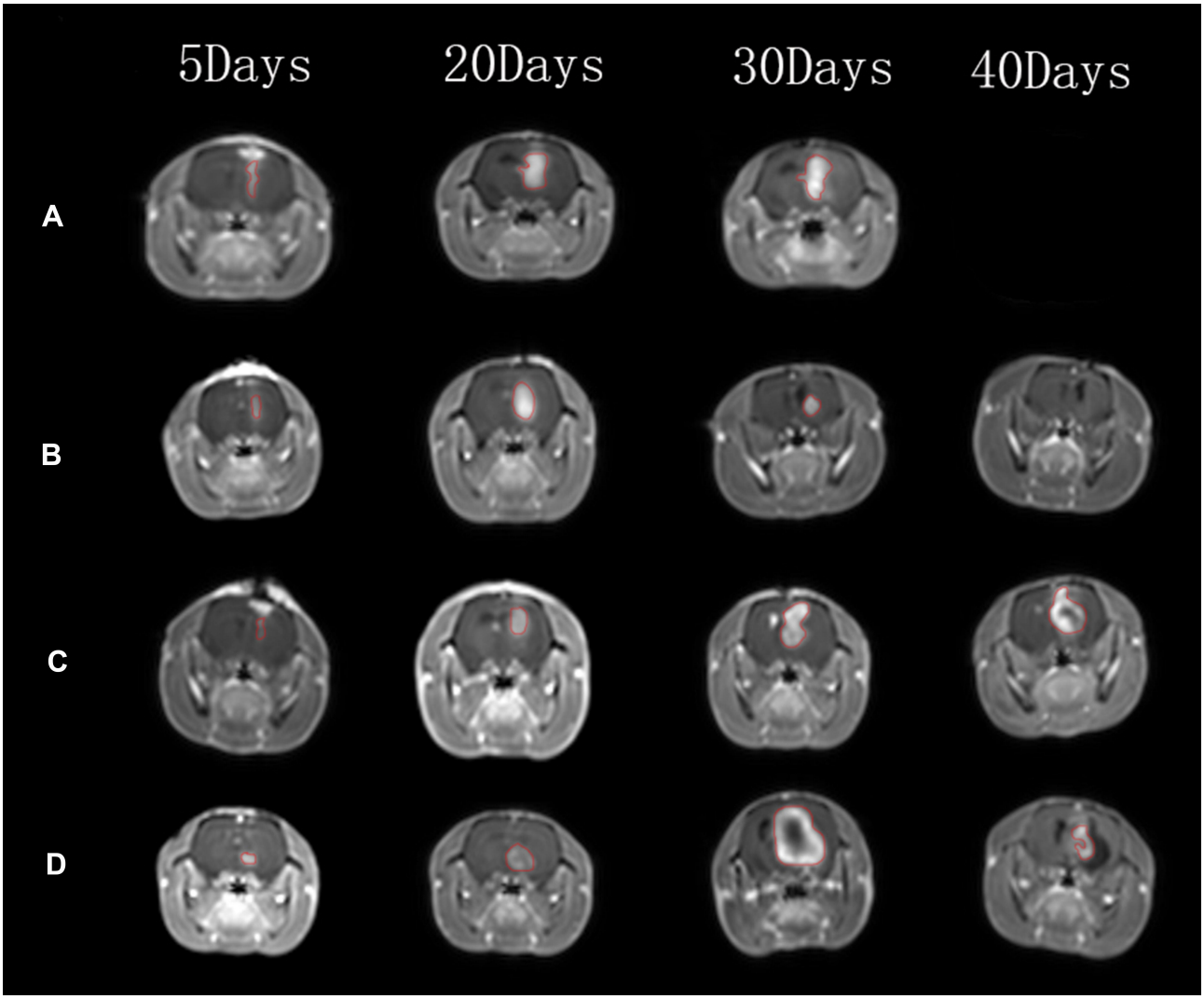

Figure 8 Representative magnetic resonance images (MRIs) of the (**A**) tumor group, (**B**) 9L + C6 treatment group, (**C**) thymosin treatment group, and (**D**) 9L + C6 + thymosin treatment group at 5, 20, 30, and 40 days after remodeling. Because the tumor group rats died before day 40, end-stage MRI on Day 26 is provided for the Day 30 image.

Hybrid Vaccine Treatment-Stimulated IL-10 and IL-2 Secretion

To assess the in vivo efficacy of the vaccine, peripheral blood IL-10 and IL-2 level for the five treatment groups was measured using ELISA. The IL-10 level was increased in the tumor and 9L + C6 treatment groups ($p < 0.05$), slightly higher in the 9L + C6 + thymosin treatment group, and remained unchanged in the thymosin treatment group compared with the blank control group (Figure 10A). The 9L + C6, thymosin, and 9L + C6 + thymosin treatment groups were able to effectively stimulate the release of IL-2 compared with the blank control group (Figure 10B; $p < 0.05$). However, no significant difference was observed in the IL-2 expression level between the tumor and blank control groups (Figure 10B).

Hybrid Vaccine Treatment-Induced Increase in the Infiltration of CD4+ T, CD8+ T, and CD161+ NK Cells in Rat Glioma Tissue

We subsequently assessed the infiltration (relative abundance) of CD4+ T, CD8+ T, and CD161+ NK cells in rat glioma tissue of the five treatment groups. Increased infiltration of $CD4^+$ T cells was observed in the 9L + C6, thymosin, and 9L + C6 + thymosin treatment groups compared with the blank control group (Figure 11A; $p < 0.05$). No significant difference in the abundance of CD4+ T cells was observed in the tumor group. The abundance of CD8+ T cells was increased in the 9L + C6 and 9L + C6 + thymosin treatment groups compared with the blank control group (Figure 11B;

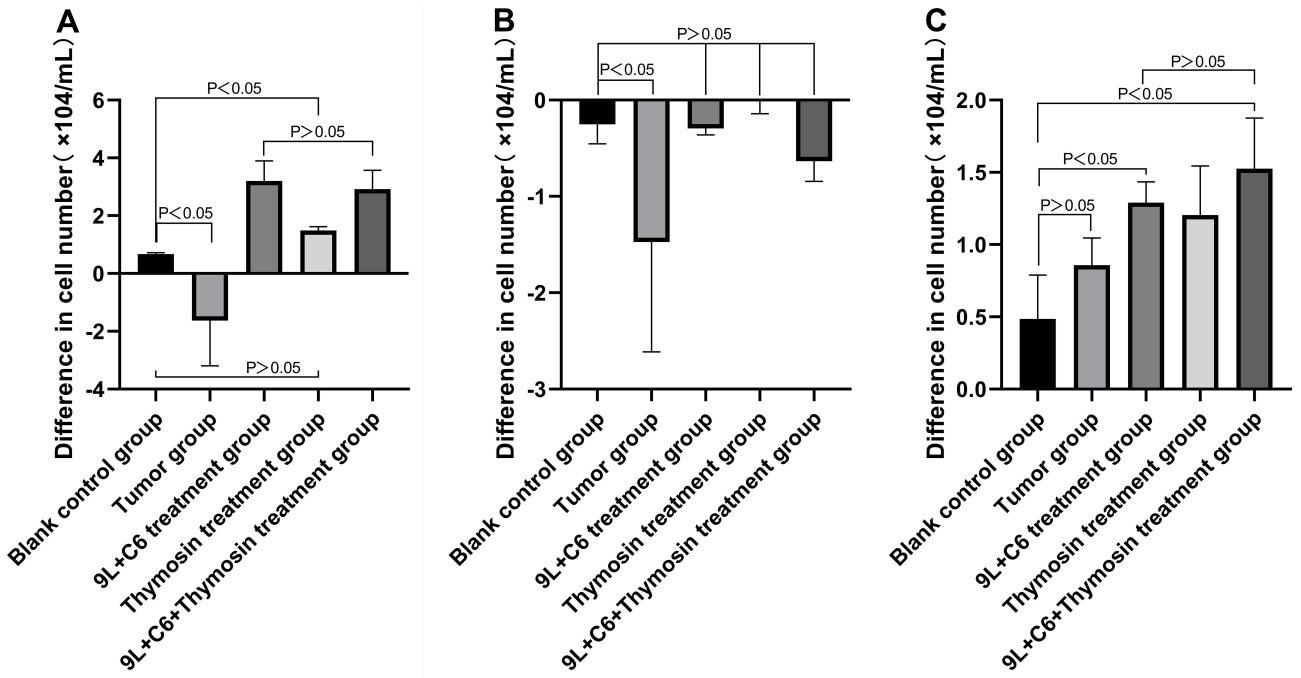

Figure 9 Graphs showing the difference in pre- and post-treatment peripheral blood cell count for (**A**) CD4+ T cells, (**B**) CD8+ T cells, and (**C**) NK cells for the five treatment groups. Data are presented as mean ± standard deviation (SD) of three independent experiments (n = 3). One-way ANOVA statistical test was performed for comparisons among groups.

$p < 0.05$). No significant change in $CD8^+$ T-cell abundance was observed in the tumor and thymosin treatment groups (Figure 11B). Higher infiltration of CD161+ NK cells was observed in the 9L + C6 and 9L + C6 + thymosin treatment groups than in the blank control group (Figure 11C; $p < 0.05$). No significant change was observed in the infiltration of CD161+ NK cells in the tumor and thymosin treatment groups (Figure 11C).

Discussion

In this study, we evaluated the in vitro and in vivo efficacy of a tumor lysate-based glioma vaccine and demonstrated the feasibility of its use as an immunotherapeutic agent. First, we tested the effect of autologous 9L glioma cell lysate and allogeneic C6 glioma cell lysate, individually and combined, as immunogens of DC maturation. Both types of glioma cell lysates were able to activate DCs individually, as well as in combination, as was evident from the detection of the characteristic DC surface markers. Next, we assessed the ability of activated DCs to induce T-cell proliferation in DC/T-cell co-cultures to determine the optimal DC-to-T-cell ratio for the vaccine formulation, which was found to be 1:20. Subsequently, we determined the cytolytic effect of the vaccine on glioma cells. We found increased glioma cell apoptosis, reduced glioma cell viability, and increased chemokine and cytokine secretion from T cells for all the three glioma-to-vaccine ratios. The hybrid 9L + C6 cell lysate vaccine demonstrated the best in vitro efficacy, providing credence to our hypothesis of designing a multi-epitope tumor vaccine based on the theoretical molecular simulation principle. Then, we proceeded to evaluate the in vivo efficacy of this hybrid vaccine on 9L/F344 rat glioma models. We randomly allocated the 40 rats into five treatment groups of eight rats each and subjected them to respective treatments: blank, tumor, 9L + C6 (vaccine), thymosin, and 9L + C6 + thymosin (vaccine + thymosin). The 9L + C6 treatment group demonstrated longer survival duration, lower intracranial tumor volume, higher peripheral blood CD4+ and NK cell count, greater IL-10 and IL-2 cytokine level, and higher immune cell (CD4+ T, CD8+ T, and NK cells) infiltration in rat glioma tissue. Although the peripheral CD8+ T-cell level did not exactly increase after vaccine treatment, it was higher than that of the tumor group, which demonstrated reduced peripheral CD8+ T-cell count. This indicates the ability of the vaccine to activate the immune system and limit glioma progression. We found that thymosin, a hormone that stimulates T-cell maturation,[23] demonstrated weak antitumor effect in the rat glioma models. A slight increase in

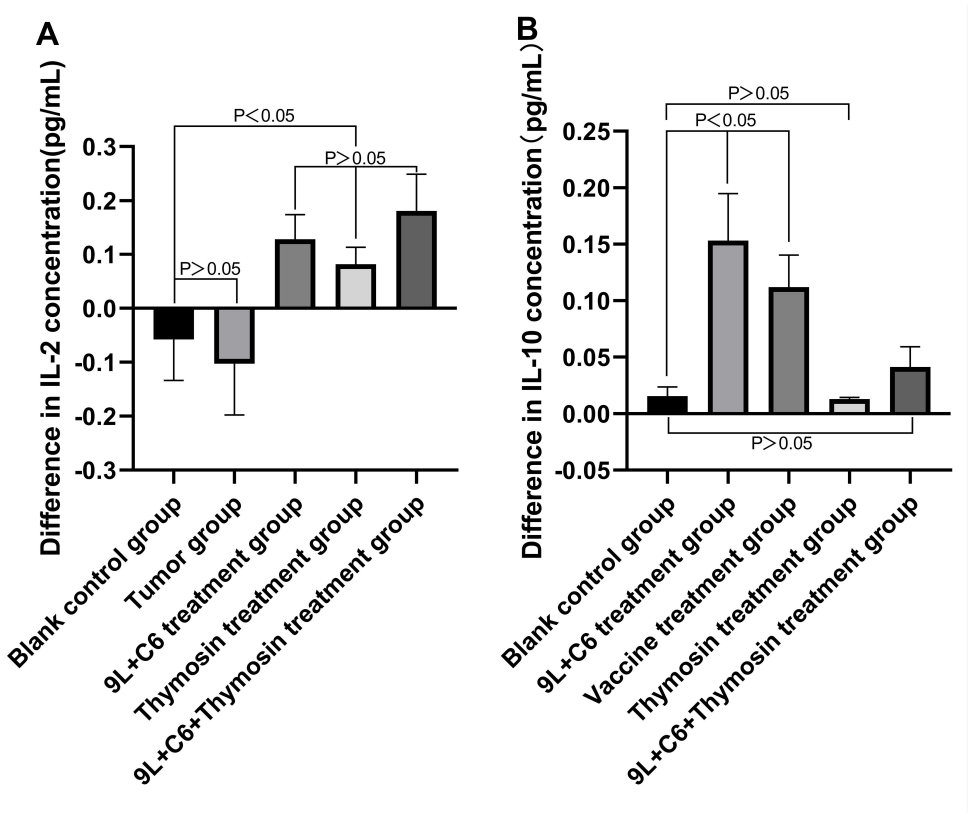

Figure 10 Graphs showing the secretion levels of (**A**) IL-2 and (**B**) IL-10 cytokines in the five treatment groups, as detected using ELISA. Data are presented as mean ± standard deviation (SD) of three independent experiments (n = 3). One-way ANOVA statistical test was performed for comparisons among groups.

peripheral and tumor-infiltrating CD4+ T cells, but not in CD8+ T and NK cells, was observed in the thymosin treatment group. In addition, IL-2, not IL-10, cytokine secretion was observed following thymosin treatment. Furthermore, the effect of thymosin in combined therapy did not appear to strengthen the antiglioma efficacy of the vaccine. The immune-promoting effect was not as desired, possibly because thymosin enhances immunity in a non-specific manner.

Allogeneic and autologous tumor-associated immunogens consist of T-cell epitopes that mediate antitumor immune responses such as engagement and activation of T cells and upregulation of MHC cell-surface expression on DCs.[24] In this study, we demonstrated the effect of these two immunogen types on DC maturation and T-cell proliferation stimulation. To detect tumor antigen-induced DC activation, we assessed a panel of typical mature DC surface markers. The CD80 and CD86 cell-surface markers, which belong to the immunoglobulin superfamily and are critical for T-cell activation, can be simultaneously stimulated by their respective ligands CD28 and CTLA-4, found on the surface of T cells.[25] Increased expression of CD80 and CD86 on the surface of DCs potentiates the first wave of T-cell activation and initiates the immune response.[25] CD86 primarily induces the differentiation of helper T cells and maintains and enhances the antigen-induced inflammatory response. OX62 is another mature DC marker that is primarily expressed on rat CD4+ and CD4− DCs.[26] CD11c, a classical marker of mature DCs and a member of the β2-integrin family, can regulate the proliferation and function of CD4+ and CD8+ T cells.[27–30] The marker is highly expressed on the surface of most DCs, monocytes, and macrophages but is less abundant on the surface of plasmacytoid DCs.[31] However, high numbers of CD11c+ DCs suppress the immune system and reduce the antitumor ability.[32] In this study, we observed increased levels of the selected six-panel cell surface markers, indicating the successful activation of DCs by the treatments tested. This allowed us to continue to determine the DC-to-T-cell target ratio for DC-based vaccine formulation.

IFN-γ cytokine, the classical indicator of T-cell activation, can stimulate activation of the downstream chemokine MCP-2.[33] Although the allogeneic C6 cell lysate and

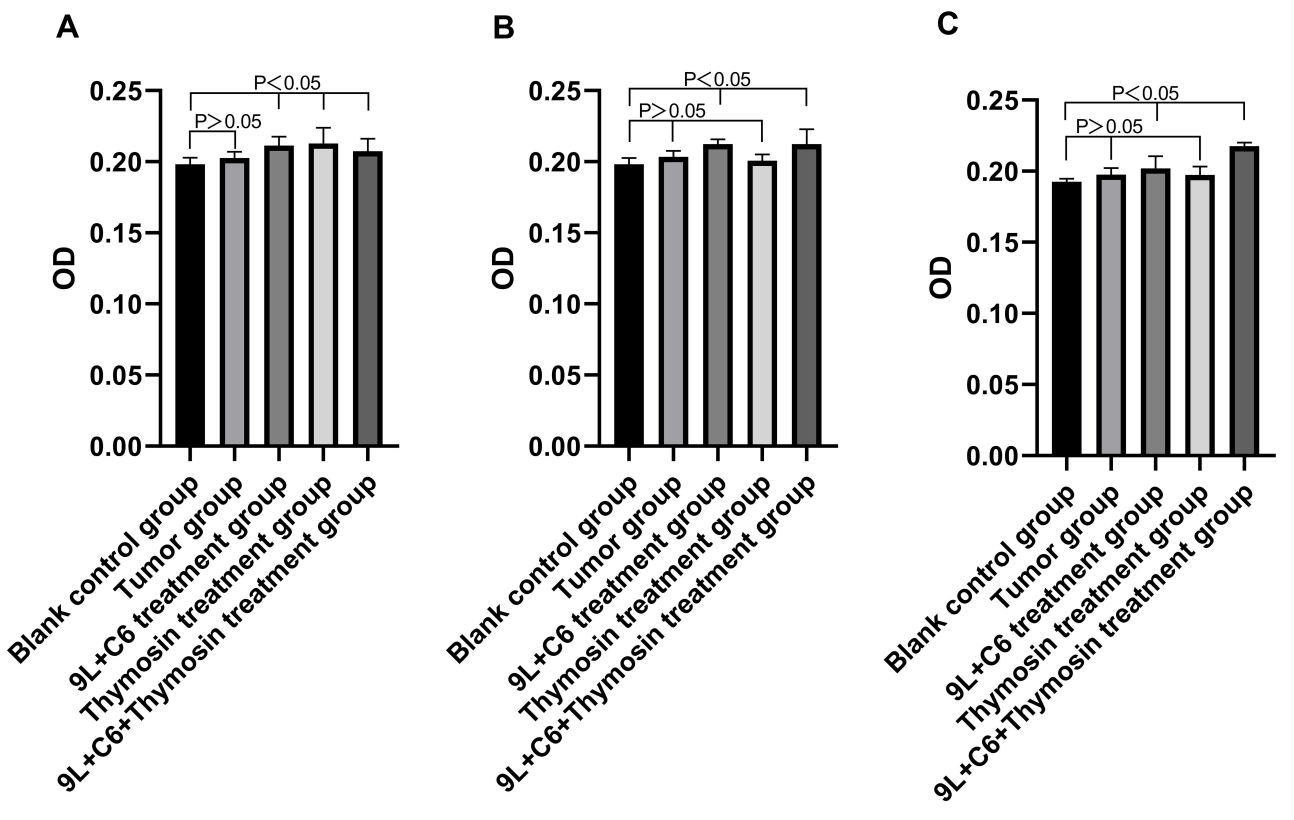

Figure 11 Immunohistochemical images of the abundance of (**A**) CD4+ T cells, (**B**) CD8+ T cells, and (**C**) CD161+ natural killer (NK) cells in rat tumor tissues for the five treatment groups.

9L + C6 cell lysate hybrid vaccines were able to induce the release of MCP-2 and IFN-γ, the effect appeared to be modest at best. Moreover, the autologous 9L cell lysate vaccine alone could not stimulate MCP-2 and IFN-γ secretion from T cells. We speculate that our in vitro conditions could not fully replicate the complex in vivo immune environment. In our experiment, we mainly focused on dendritic, glioma, and T cells, although tumor immunity involves the coordinated response of a myriad of immune cell populations.[34] Thus, this limitation could be the reason for the observed poor induction of chemokine and cytokine release from T cells by DCs. Nonetheless, because the hybrid vaccine could successfully induce cytokine and chemokine release, thus indicating its in vitro efficacy, we decided to continue with in vivo efficacy evaluation.

Glioma is typically accompanied by immune surveillance failure due to immunosuppression.[35] In the in vivo rat glioma models, the tumor group demonstrated decreased peripheral and tumor-infiltrating CD4+ T cells, whereas the vaccine-treatment group demonstrated increased levels of these cells. This finding suggests that the hybrid vaccine could override the immunosuppression induced by gliomas and activate the immune response. Moreover, although no significant increase was observed in peripheral CD8+ T cells, elevated levels of tumor-infiltrating CD8+ T cells indicate enhanced cellular immunity. Increased peripheral and tumor-infiltrating NK cells observed in the vaccine- and combined-treatment groups were also consistent with the increase in the CD4+ and CD8+ T immune cells. Moreover, increased NK-cell infiltration indicates strengthened immunity, considering their role as tumor-killing cells.

IL-10 inhibits the activation and effector functions of DCs, macrophages, and T cells; regulates the growth and differentiation of immune cells; and downregulates the expression of Th1 cytokines and MHC-II antigens on macrophages and monocytes.[36,37] Although IL-10 functions in immunosuppression and inflammation inhibition, it has demonstrated pro-inflammatory and antitumor effects. In gliomas, IL-10 reportedly upregulated the immune checkpoint programmed cell death ligand PD-L1 in circulating

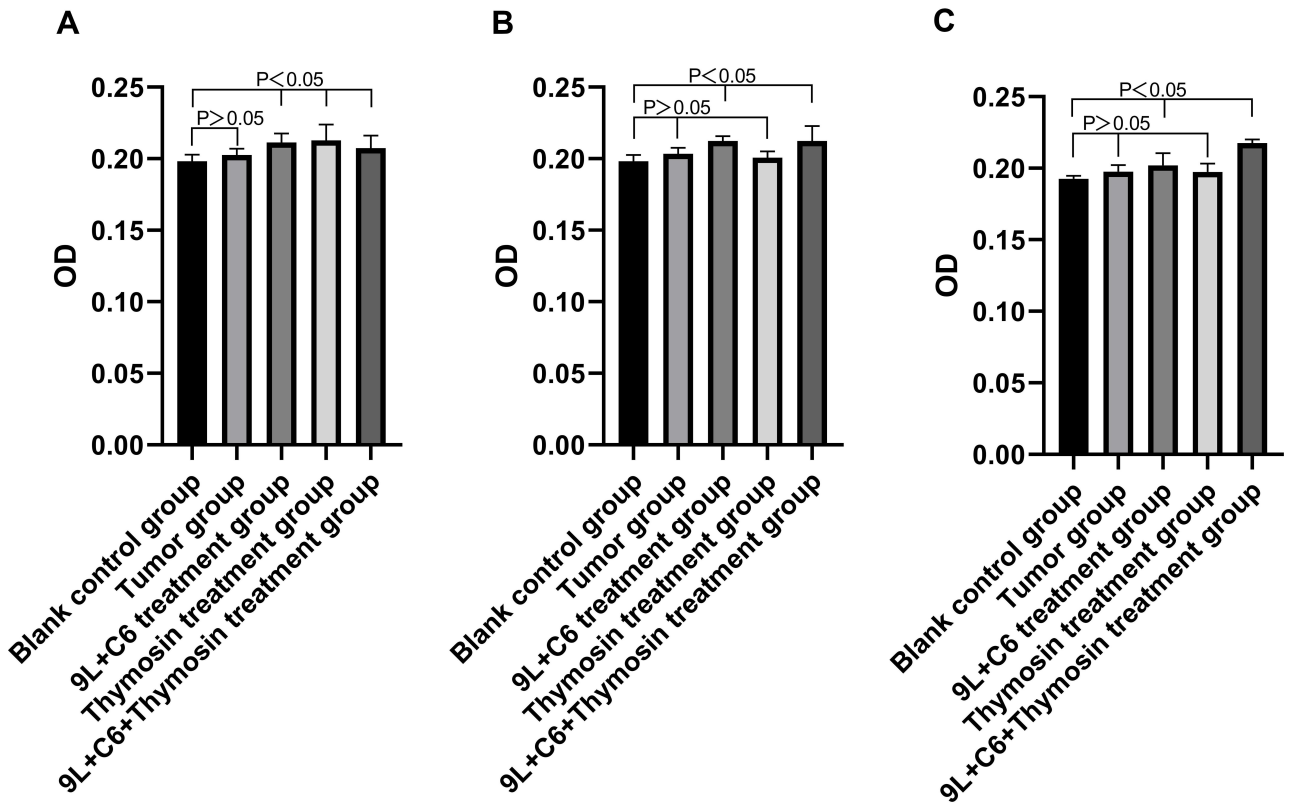

Figure 12 Histograms showing the optical density (OD) levels of (**A**) CD4, (**B**) CD8, and (**C**) CD161 in the five treatment groups. Data are presented as mean ± standard deviation (SD) of three independent experiments (n = 3). One-way ANOVA statistical test was performed for comparisons among groups.

monocytes and tumor-associated macrophages[38] and promoted T-cell proliferation to inhibit glioma progression.[39] In addition, IL-10 induced macrophages to produce antiangiogenic cytokines and promote antitumor NK-cell responses.[36] Considering its dual role, we cannot reliably use the IL-10 secretion level as a marker to assess the efficacy of glioma treatment. In contrast, IL-2, known to induce anticancer effects such as T-cell proliferation and trigger innate and adaptive immunity,[39,40] can be used to assess the efficacy of the vaccine. IL-2 levels increased in the vaccine-, thymosin-, and combined-treatment groups, indicating the effectiveness of all three treatments. However, the modest increase in IL-2 level in the thymosin-treatment group reflects partial immune enhancement by thymosin.

Future follow-up research regarding the effect of vaccine administration on glioma cell invasion, immune cell subtypes and cytokines, T-cell sequestration in the bone marrow, and circulating immune cells in the brain tissue, as well as the effect of vaccine treatment on different tumor models, is warranted. In conclusion, we demonstrated good in vitro and in vivo antiglioma efficacy of the tumor cell lysate-based vaccine. Our study proposes the potential clinical application of the vaccine that was developed based on the principle of molecular dynamics in glioma immunotherapy. This molecular simulation-based hybrid vaccine will add value to the current knowledge on vaccine immunotherapy.

Funding

This research was financially supported by Sichuan Science and Technology Support Plan Project (2013SZZ002); Luzhou Municipal Government-Southwest Medical University Joint Scientific Research Special Fund Plan Project (14ZC0071-LH09); Luzhou Municipal Government-Southwest Medical University Joint Scientific Research Special Fund Plan Project (2016LZXNYD-G03); Southwest Medical University Youth Fund Project (2013ZRQN068); and Sichuan Provincial Health and Family Planning Commission Member Association Scientific Research Project (Universal Application Project; 16PJ557).

Disclosure

The authors report no conflicts of interest for this work.

References

1. Eder K, Kalman B. The Dynamics of Interactions Among Immune and Glioblastoma Cells[J]. *Neuromolecular Med*. 2015;17(4):335–352. doi:10.1007/s12017-015-8362-x
2. Hanif F, Muzaffar K, Perveen K, et al. Glioblastoma Multiforme: A review of its epidemiology and pathogenesis through clinical presentation and treatment. *Asian Pac J Cancer Prev*. 2017;18(1):3–9. doi:10.22034/APJCP.2017.18.1.3
3. Chinnaiyan P, Won M, Wen PY, et al. A randomized Phase II study of everolimus in combination with chemoradiation in newly diagnosed glioblastoma: results of NRG Oncology RTOG 0913. *Neuro Onco*. 2018;20(5):666–673. doi:10.1093/neuonc/nox209
4. Zhang J, Guan M, Wang Q, et al. Single-cell transcriptome-based multilayer network biomarker for predicting prognosis and therapeutic response of gliomas. *Brief Bioinform*. 2019;21(3):1080–1097. doi:10.1093/bib/bbz040
5. Goel G, Sun W. Cancer immunotherapy in clinical practice-the past, present, and future[J]. *Clin Cancer Res*. 2014;33(9):445–457.
6. Roche PA, Cresswell P. Antigen processing and presentation mechanisms in myeloid cells. *Microbiol Spectr*. 2016;4(3). doi:10.1128/microbiolspec.MCHD-0008-2015
7. Mastelic-Gavillet B, Balint K, Boudousquie C, et al. Personalized dendritic cell vaccines – recent breakthroughs and encouraging clinical results. *Front Immunol*. 2019;10:766. doi:10.3389/fimmu.2019.00766
8. Gonzalez FE, Gleisner A, Falcón-Beas F, et al. Tumor cell lysates as immunogenic sources for cancer vaccine design. *Hum Vaccin Immunother*. 2015;10(11):3261–3269. doi:10.4161/21645515.2014.982996
9. Palez CR, De Palma M. Engineering dendritic cell vaccines to improve cancer immunotherapy. *Nat Commun*. 2019;10(1):5408. doi:10.1038/s41467-019-13368-y
10. Rajput MKS, Kesharwani SS, Kumar S, et al. Dendritic Cell-Targeted Nanovaccine Delivery System Prepared With an Immune-Active Polymer. *ACS Appl Mater Interfaces*. 2018;10(33):27589–27602. doi:10.1021/acsami.8b02019
11. Kumar S, Kesharwani SS, Kuppast B, et al. Pathogen-mimicking vaccine delivery system designed with a bioactive polymer (inulin acetate) for robust humoral and cellular immune responses. *J Control Release*. 2017;261:263–274. doi:10.1016/j.jconrel.2017.06.026
12. Kumar S, Kesharwani SS, Kuppast B, et al. Discovery of Inulin Acetate as a Novel Immune-Active Polymer and Vaccine Adjuvant: synthesis, Material Characterization, and Biological Evaluation as a Toll-Like receptor-4 Agonist. *J Mater Chem B*. 2016;4(48):7950–7960. doi:10.1039/C6TB02181F
13. Hu X, Wu T, Qin X, et al. Tumor Lysate-Loaded Lipid Hybrid Nanovaccine Collaborated with an Immune Checkpoint Antagonist for Combination Immunotherapy. *Adv Healthc Mater*. 2019;8(1):e1800837. doi:10.1002/adhm.201800837
14. Benci JL, Xu B, Qiu Y, et al. Tumor Interferon Signaling Regulates a Multigenic Resistance Program to Immune Checkpoint Blockade. *Cell*. 2016;167(6):1540–1554. doi:10.1016/j.cell.2016.11.022
15. Zaretsky JM, Garcia-Diaz A, Shin DS. Mutations Associated with Acquired Resistance to PD-1 Blockade in Melanoma. *N Engl J Med*. 2016;375(9):819–829. doi:10.1056/NEJMoa1604958
16. Im SJ, Hashimoto M, Gerner MY, et al. Defining CD8+ T cells that provide the proliferative burst after PD-1 therapy. *Nature*. 2016;537(7620):417–421. doi:10.1038/nature19330
17. Huang AC, Postow MA, Orlowski RJ, et al. T-cell invigoration to tumour burden ratio associated with anti-PD-1 response. *Nature*. 2017;545(7652):60–65. doi:10.1038/nature22079
18. Wartewig T, Kurgyis Z, Keppler S, et al. PD-1 is a haploinsufficient suppressor of T cell lymphomagenesis. *Nature*. 2017;552(7683):121–125. doi:10.1038/nature24649
19. Sondak VK, et al. Allogeneic and autologous melanoma vaccines: where have we been and where are we going? *Clin Cancer Res*. 2006;12(7 Pt 2):2337s–2341s. doi:10.1158/1078-0432.CCR-05-2555
20. Dong B, Wang L, Nie S. Anti-glioma effect of intracranial vaccination with tumor cell lysate plus flagellin in mice. *Vaccine*. 2018;36(52):8148–8157. doi:10.1016/j.vaccine.2018.04.053
21. Xiaoqing F, Wei, Y, Zheng, D, et al. Triplet anti-tumor therapy based on thumosinα-1 attenuates of hepatoma and serum alpha-fetoprotein level in rat hepatoma model[J]. *Chin J Cell Mol Immunol*. 2015;31(6):744–748.
22. Abedelahi A, Hasanzadeh H, Hadizadeh H, et al. Morphometric and volumetric study of caudate and putamen nuclei in normal individuals by MRI: effect of normal aging, gender and hemispheric differences[J]. *Pol J Radiol*. 2013;78(3):7–14. doi:10.12659/PJR.889364
23. Morita T, Hayashi K. Tumor progression is mediated by thymosin-b4 through a TGFb/MRTF signaling axis. *Mol Cancer Res*. 2018;16(5):880–893. doi:10.1158/1541-7786.MCR-17-0715
24. Altmann DM. A Nobel prize-worthy pursuit: cancer immunology and harnessing immunity to tumour neoantigens. *Immunology*. 2018;155(3):283–284. doi:10.1111/imm.13008
25. Lim TS, Goh JKH, Mortellaro A, et al. CD80 and CD86 differentially regulate mechanical interactions of T-cells with antigen-presenting dendritic cells and B-cells. *PLoS One*. 2012;7(9):e45185. doi:10.1371/journal.pone.0045185
26. Brissette-Storkus CS, Kettel JC, Whitham TF, et al. Flt-3 ligand (FL) drives differentiation of rat bone marrow-derived dendritic cells expressing OX62 and/or CD161 (NKR-P1). *J Leukoc Biol*. 2002;71(6):941–949.
27. Wu J, Wu H, An J, et al. Critical role of integrin CD11c in splenic dendritic cell capture of missing-self CD47 cells to induce adaptive immunity. *Proc Natl Acad Sci USA*. 2018;115(26):6786–6791. doi:10.1073/pnas.1805542115
28. Takeda Y, Azuma M, Matsumoto M, et al. Tumoricidal efficacy coincides with CD11c up-regulation in antigen-specific CD8(+) T cells during vaccine immunotherapy. *J Exp Clin Cancer Res*. 2016;35(1):143. doi:10.1186/s13046-016-0416-x
29. Qualai J, Li L-X, Cantero J, et al. Expression of CD11c Is Associated with Unconventional Activated T Cell Subsets with High Migratory Potential. *PLoS One*. 2016;11(4):e0154253. doi:10.1371/journal.pone.0154253
30. Castro F, Tutt A, White A, et al. CD11c provides an effective immunotarget for the generation of both CD4 and CD8 T cell responses[J]. *Eur J Immunol*. 2008;38(8):2263–2273. doi:10.1002/eji.200838302
31. Merad M, Sathe P, Helft J, et al. The Dendritic Cell Lineage: ontogeny and Function of Dendritic Cells and Their Subsets in the Steady State and the Inflamed Setting. *Annu Rev Immunol*. 2013;31(1):563–604. doi:10.1146/annurev-immunol-020711-074950
32. Gardner A, Ruffell B. Dendritic cells and cancer immunity. *Trends Immunol*. 2016;37(12):855–865. doi:10.1016/j.it.2016.09.006
33. Lalvani A, Millington KA. T-cell interferon-gamma release assays: can we do better? *Eur Respir J*. 2008;32(6):1428–1430. doi:10.1183/09031936.00148308
34. Gonzalez H, Hagerling C, Werb Z, et al. Roles of the immune system in cancer: from tumor initiation to metastatic progression. *Genes Dev*. 2018;32(19–20):1267–1284. doi:10.1101/gad.314617.118
35. Lehtipuro S, Nykter M, Granberg KJ, et al. Modes of immunosuppression in glioblastoma microenvironment. *Oncotarget*. 2019;10(9):920–921. doi:10.18632/oncotarget.26643
36. Perng P, Lim M. Immunosuppressive mechanisms of malignant gliomas: parallels at non-CNS sites. *Front Oncol*. 2015;5:153. doi:10.3389/fonc.2015.00153
37. Mittal SK, Roche PA. Suppression of antigen presentation by 1L-10. *Curr Opin Immunol*. 2015;34:22–27. doi:10.1016/j.coi.2014.12.009
38. Bloch O, Crane CA, Kaur R, Safaee M, Rutkowski MJ, Parsa AT. Gliomas promote immunosuppression through induction of B7-H1 expression in tumor-associated macrophages. *Clin Cancer Res*. 2013;19(12):3165–3175. doi:10.1158/1078-0432.CCR-12-3314

39. Li X, Lu P, Li B, et al. Interleukin 2 and interleukin 10 function synergistically to promote $CD8^+$ T cell cytotoxicity, which is suppressed by regulatory T cells in breast cancer. *Int J Biochem Cell Biol*. 2017;87:1–7. doi:10.1016/j.biocel.2017.03.003

40. Qiao, HB, Li, J, Lv, L, et al. The effects of interleukin 2 and rAd-p53 as a treatment for glioblastoma[J]. *Mol Med Rep*. 2018;17(3):4853–4859. doi:10.3892/mmr.2018.8408